Video Article

Dissection of Hippocampal Dentate Gyrus from Adult Mouse

Hideo Hagihara[1,2], Keiko Toyama[1,2], Nobuyuki Yamasaki[2,3], Tsuyoshi Miyakawa[1,2,4,5]

[1]Division of Systems Medical Science, Institute for Comprehensive Medical Science, Fujita Health University
[2]Japan Science and Technology Agency, Core Research for Evolutionary Science and Technology (CREST)
[3]Department of Psychiatry, Kyoto Prefectural University for Medicine
[4]Genetic Engineering and Functional Genomics Group, Horizontal Medical Research Organization, Kyoto University Faculty of Medicine
[5]Center for Genetic Analysis of Behavior, National Institute for Physiological Sciences, National Institutes of Natural Sciences

Correspondence to: Tsuyoshi Miyakawa at miyakawa@fujita-hu.ac.jp

URL: http://www.jove.com/details.php?id=1543

DOI: 10.3791/1543

Citation: Hagihara H., Toyama K., Yamasaki N., Miyakawa T. (2009). Dissection of Hippocampal Dentate Gyrus from Adult Mouse. JoVE. 33. http://www.jove.com/details.php?id=1543, doi: 10.3791/1543

Abstract

The hippocampus is one of the most widely studied areas in the brain because of its important functional role in memory processing and learning, its remarkable neuronal cell plasticity, and its involvement in epilepsy, neurodegenerative diseases, and psychiatric disorders. The hippocampus is composed of distinct regions; the dentate gyrus, which comprises mainly granule neurons, and Ammon's horn, which comprises mainly pyramidal neurons, and the two regions are connected by both anatomic and functional circuits. Many different mRNAs and proteins are selectively expressed in the dentate gyrus, and the dentate gyrus is a site of adult neurogenesis; that is, new neurons are continually generated in the adult dentate gyrus. To investigate mRNA and protein expression specific to the dentate gyrus, laser capture microdissection is often used. This method has some limitations, however, such as the need for special apparatuses and complicated handling procedures. In this video-recorded protocol, we demonstrate a dissection technique for removing the dentate gyrus from adult mouse under a stereomicroscope. Dentate gyrus samples prepared using this technique are suitable for any assay, including transcriptomic, proteomic, and cell biology analyses. We confirmed that the dissected tissue is dentate gyrus by conducting real-time PCR of dentate gyrus-specific genes, tryptophan 2,3-dioxygenase (TDO2) and desmoplakin (Dsp), and Ammon's horn enriched genes, Meis-related gene 1b (Mrg1b) and TYRO3 protein tyrosine kinase 3 (Tyro3). The mRNA expressions of TDO2 and Dsp in the dentate gyrus samples were detected at obviously higher levels, whereas Mrg1b and Tyro3 were lower levels, than those in the Ammon's horn samples. To demonstrate the advantage of this method, we performed DNA microarray analysis using samples of whole hippocampus and dentate gyrus. The mRNA expression of TDO2 and Dsp, which are expressed selectively in the dentate gyrus, in the whole hippocampus of alpha-CaMKII+/- mice, exhibited 0.037 and 0.10-fold changes compared to that of wild-type mice, respectively. In the isolated dentate gyrus, however, these expressions exhibited 0.011 and 0.021-fold changes compared to that of wild-type mice, demonstrating that gene expression changes in dentate gyrus can be detected with greater sensitivity. Taken together, this convenient and accurate dissection technique can be reliably used for studies focused on the dentate gyrus.

Protocol

Dissection of hippocampal dentate gyrus

1. In a deeply anesthetized mouse, carefully dissect the brain out from the skull and place it into ice-cold phosphate-buffered saline (PBS).
2. In a Petri dish containing ice-cold PBS, cut the brain along the longitudinal fissure of the cerebrum using a surgical knife, and cut off the regions posterior to lambda (midbrain, hindbrain, and cerebellum).
3. Place the cerebral hemisphere medial side up and, using forceps, carefully remove the diencephalon (thalamus and hypothalamus) under a dissection microscope. This will expose the medial side of the hippocampus, allowing for visualization of the dentate gyrus. The dentate gyrus is distinguishable from Ammon's horn by the gaps between them. Injury to the hippocampus or surrounding area will make it more difficult to isolate the dentate gyrus.
4. Insert a sharp needle-tip (e.g., 27-gauge needle) into each side of the dentate gyrus (boundaries of the dentate gyrus and Ammon's horn; Figure 1), and slide the needles superficially along the septo-temporal axis of hippocampus to isolate the dentate gyrus.
5. Pick up the isolated dentate gyrus using a needle or forceps and place it in a sample tube. The thus-obtained dentate gyrus tissue sample can be used immediately for any assay or stored in a deep-freezer for later use.
6. Isolate the dentate gyrus from the other cerebral hemisphere using the same method.

Quantitative real-time PCR

The dentate gyrus was isolated using the above-mentioned method and the remaining hippocampus was dissected out as the Ammon's horn sample from wild-type mice. Real-time PCR of beta-actin, TDO2, Dsp, Mrg1b and Tyro3 were performed with the dentate gyrus and the Ammon's horn samples as described previously[1]. Primers 5'-CTGGCGAGATCACGATGACG and 5'-AAGCTACGCTGTTGTCTAACC were used for Mrg1b, and GCCTCCAAATTGCCCGTCA and 5'-CCAGCACTGGTACATGAGATCA for Tyro3.

Microarray analysis

Microarray experiments were performed with male wild-type mice and mice heterozygous for the alpha-isoform of calcium/calmodulin-dependent protein kinase II (alpha-CaMKII+/- mice) as described previously[1]. Briefly, RNA isolated from the whole hippocampus or dentate gyrus of wild-type and mutant mice was hybridized with a Mouse Genome 430 2.0 Array (Affymetrix, Santa Clara, CA), and each GeneChip was scanned by an Affymetrix GeneChip Scanner 3000 (GCS3000). GeneChip analysis was performed with Microarray Analysis Suite version 5.0.

Discussion

The dentate gyrus occupies approximately 25% to 30% of the volume of the hippocampal formation[2,3]. It has a unique cell composition and plays crucial roles in various brain functions. Therefore, techniques to isolate the dentate gyrus are useful for analyzing the events that occur specifically in this region.

Here, we demonstrated a procedure to efficiently dissect the dentate gyrus from adult mouse hippocampus and confirmed the precision of the technique. First, histologic study revealed that the dentate gyrus was separated without contamination by other regions (Figure 1), indicating that a pure dentate gyrus sample can be prepared.

Second, we confirmed that the dissected tissue is dentate gyrus by conducting real-time PCR of dentate gyrus-specific genes, TDO2 and Dsp, and Ammon's horn enriched genes, Mrg1b and Tyro3[4] (Figure 2). The mRNA expressions of TDO2 (p=0.000023; n's=4 and 4, respectively) and Dsp (p=0.0000030; n's=4 and 4, respectively) in the dentate gyrus samples were detected at obviously higher levels, whereas Mrg1b (p =0.000080; n's=4 and 4, respectively) and Tyro3 (p=0.00017; n's=4 and 4, respectively) were lower levels, than those in the Ammon's horn samples. Beta-actin expression levels did not differ in these samples (p=0.11; n's=4 and 4, respectively). Thus, we could check whether or not the dentate gyrus was accurately dissected out by conducting such simple real-time PCR experiments.

Third, to assess the usefulness of this dissection method, we compared the mRNA expression level of whole hippocampus with that of dentate gyrus. Whole hippocampus and dentate gyrus obtained from wild-type (n's=9 and 4, respectively) and alpha-CaMKII+/- mice (n's=18 and 4, respectively) were processed for microarray analysis, and for all genes scored, the fold-change was calculated by dividing the mutant value by the wild-type value. The results indicated that the changes in mRNA expression, especially of dentate gyrus-specific molecules such as Dsp and TDO2, were detected with up to a 5-fold increase in sensitivity in dentate gyrus samples compared to whole hippocampal samples (Table 1). We previously demonstrated that alpha-CaMKII+/- mice exhibit behaviors related to human psychiatric disorders such as working memory deficits and an exaggerated infradian rhythm[1,5]. Furthermore, morphologic and electrophysiologic features of the dentate gyrus neurons in mutant mice are strikingly similar to those of immature dentate gyrus neurons in normal rodents, indicating that the neurons in these mutant mice fail to develop to maturity[1]. The immature dentate gyrus and down-regulated expression of Dsp and TDO2 mRNA in alpha-CaMKII+/- mice are consistent with the finding that Dsp and TDO2 can be used as markers of mature granule cells in the dentate gyrus (Ohira et al., unpublished data).

Taken together, this convenient and accurate dissection technique can be reliably used for studies focused on the dentate gyrus. Dentate gyrus tissue obtained using this method is applicable to other types of analyses as well, including proteomic and cell biology analyses.

Figure 1. Verification of the isolated dentate gyrus by histologic study. A coronal section of the brain after isolating dentate gyrus was processed for Nissl staining (left panel), and a schematic diagram adapted from the mouse brain atlas6 represents the approximately the same level of the section shown in the left panel (right panel). Arrows indicate the directions of the needle-tip insertion. Scale bar, 1 mm.

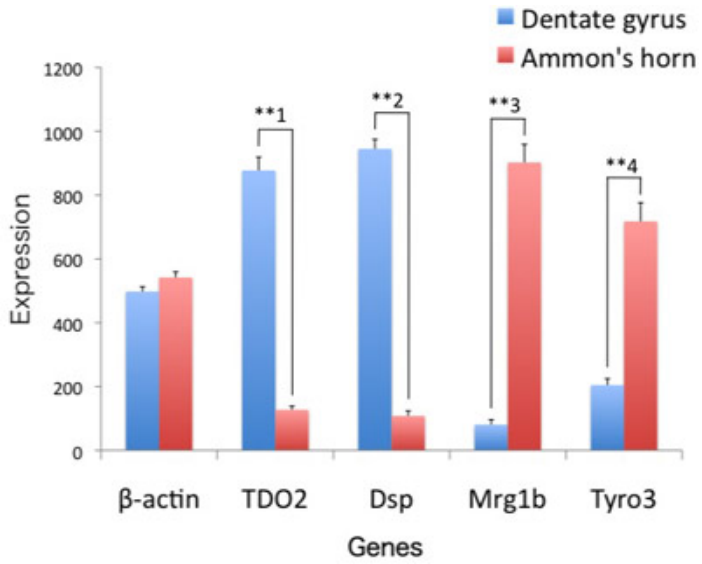

Figure 2. Verification of the isolated dentate gyrus by real-time PCR. The dentate gyrus and the Ammon s horn obtained from four wild-type mice were processed for real-time PCR of beta-actin, TDO2, Dsp, Mrg1b and Tyro3. Results are presented as means ± SEM. For statistical analysis, Student s *t* test was employed, and *p* values are followed: beta-actin, *p*=0.11; TDO2, *p*=0.000023 (**1); Dsp, *p*=0.0000030 (**2); Mrg1b, *p* =0.000080 (**3); and Tyro3, *p*=0.00017 (**4).

Table 1. Microarray analysis of whole hippocampus and dentate gyrus. Genes differentially expressed in dentate gyrus and whole hippocampus of alpha-CaMKII+/- mice were determined by calculating the fold-change from that detected in wild-type mice. Data were analyzed for statistical significance using the Student s *t* test between wild-type and alpha-CaMKII+/- mice. Among the genes whose expression exhibited *p* <0.05 in the dentate gyrus of alpha-CaMKII+/- mice compared to that of wild-type mice, the top 50 genes are listed. Note that the numbers of samples for dentate gyrus are much less than those for whole hippocampus. AffyID, Affymetrix probe identifier; CKII, alpha-CaMKII+/- mice; WT, wild-type mice.

			Dentate gyrus (*p* <0.05) WT: n=4, CKII+/-: n=4		Whole hippocampus WT: n=9, CKII+/-: n=18	
Gene Title	Genebank	AffyID	Fold change	*p* value	Fold change	*p* value
desmoplakin	AV297961	1435494_s_at	0.011018913	7.02694E-06	0.037021003	1.86126E-13
desmoplakin	AV297961	1435493_at	0.014369734	7.86747E-06	0.04232106	1.00579E-12
tryptophan 2,3-dioxygenase	AI098840	1419093_at	0.020986484	5.23546E-09	0.101037776	4.14823E-13
nephronectin	AA223007	1452106_at	0.075479901	1.05191E-08	0.234001154	1.66301E-15
nephronectin	AA223007	1452107_s_at	0.079457767	1.40433E-07	0.177974715	3.9758E-12
thyrotropin releasing hormone receptor	M59811	1449571_at	0.103105815	0.003093796	0.801412732	0.283994361
ryanodine receptor 1, skeletal muscle	X83932	1427306_at	0.104825517	3.38513E-07	0.650685017	0.000308462
nescient helix loop helix 1	NM_010916	1419533_at	9.431896	6.7979E-06	4.078815314	5.27E-11
copine family member IX	BB274531	1454653_at	9.159157	7.99492E-06	1.797304153	0.000296375
doublecortin-like kinase 3	BB326709	1436532_at	0.109336662	1.95278E-07	0.56697229	2.62633E-08
calpain 3	AF127766	1426043_a_at	0.111269769	8.07053E-06	0.370956608	2.04421E-14
Adult male corpus striatum cDNA, RIKEN full-length enriched library, clone:C030023B07 product:unclassifiable, full	BB357628	1460043_at	0.118712341	6.16926E-07	0.682339204	2.33001E-06

insert sequence						
collagen and calcium binding EGF domains 1	AV264768	1437385_at	0.124043978	3.65669E-05	0.488394112	4.05538E-06
amyloid beta (A4) precursor protein-binding, family A, member 2 binding protein	AK013520	1431946_a_at	7.7986307	1.2098E-06	2.099164713	1.67047E-06
calbindin-28K	BB177770	1456934_at	0.130255444	3.32186E-06	0.572605751	1.99157E-10
Transcribed locus	AV328597	1443322_at	0.133290835	5.43583E-06	0.562767164	7.56544E-06
neuropeptide Y receptor Y2	NM_008731	1417489_at	0.135319609	0.000113407	0.781498474	0.00394504
ras responsive element binding protein 1	BE197381	1428657_at	0.138235114	7.93691E-07	0.651220705	2.94209E-05
glial cell line derived neurotrophic factor family receptor alpha 2	BB284482	1433716_x_at	0.139062563	2.35371E-06	0.669544709	0.000214146
preproenkephalin 1	M13227	1427038_at	6.9850435	2.39074E-08	1.766018828	0.000250501
RIKEN cDNA 1810010H24 gene	BI729991	1428809_at	6.8658915	1.88516E-05	2.77573142	6.81865E-09
ryanodine receptor 1, skeletal muscle	BG793713	1457347_at	0.151364292	3.35612E-05	0.503144617	4.32907E-05
protocadherin 21	NM_130878	1418304_at	0.152671849	8.57783E-06	0.670714726	1.56309E-05
cornichon homolog 3 (Drosophila)	NM_028408	1419517_at	0.153724144	8.90755E-06	0.95780695	0.661055608
harakiri, BCL2 interacting protein (contains only BH3 domain)	BQ175572	1439854_at	0.154284407	2.0118E-05	0.56516812	4.86925E-09
carbohydrate (N-acetylgalactosamine 4-0) sulfotransferase 9	AK017407	1431897_at	0.155238951	5.37423E-06	1.14910007	0.215637733
calpain 3	AI323605	1433681_x_at	0.160871988	1.07655E-05	0.477164757	1.33753E-11
zinc finger, CCHC domain containing 5	BQ126004	1437355_at	0.161812078	3.08262E-06	0.421252632	0.01152969
loricrin	NM_008508	1448745_s_at	0.165129967	1.86362E-05	0.639733409	0.000729772
spondin 1, (f-spondin) extracellular matrix protein	BC020531	1451342_at	0.168035879	6.67867E-07	0.821042412	0.023650765
RIKEN cDNA A930035E12 gene	AV348640	1429906_at	5.9086795	1.747E-07	1.470383201	0.104085454
BB247294 RIKEN full-length enriched, 7	BB247294	1447907_x_at	5.9047494	1.04931E-05	1.968147585	0.00010636

days neonate cerebellum Mus musculus cDNA clone A730018G18 3', mRNA sequence.						
FERM domain containing 3	BB099015	1437075_at	5.860216	0.000345581	2.780297178	1.83072E-06
neuronal pentraxin 2 /// hypothetical protein LOC100044234	NM_016789	1420720_at	5.7568517	1.34227E-06	2.652516957	0.000206279
Transcribed sequences	BG076361	1460101_at	5.657735	2.5015E-06	1.296248831	0.22870031
spondin 1, (f-spondin) extracellular matrix protein	BC020531	1424415_s_at	0.17783576	1.01658E-06	0.836181248	0.001380141
calbindin-28K	BB246032	1448738_at	0.180317904	1.35961E-05	0.647334052	4.12268E-09
MARCKS-like 1	AV110584	1437226_x_at	0.186235935	1.47067E-06	0.499291387	2.34984E-08
matrilin 2	BB338441	1455978_a_at	0.187783528	6.19122E-05	0.8967688	0.282337853
matrilin 2	BC005429	1419442_at	0.188195795	0.000105295	0.915528892	0.35282097
spondin 1, (f-spondin) extracellular matrix protein	BQ175871	1442613_at	0.189956563	9.41195E-06	0.861033222	0.1394266
arrestin 3, retinal	NM_133205	1450329_a_at	5.2130346	2.90599E-05	3.944218329	1.07437E-07
RIKEN cDNA A330050F15 gene	AV325555	1457558_at	0.19186781	0.000119342	0.660282035	2.47342E-05
contactin 3	BB559510	1438628_x_at	0.194404608	4.08641E-07	0.918742591	0.022545297
calbindin-28K	BB246032	1417504_at	0.196381321	2.24182E-05	0.619305124	3.6222E-06
gastrin releasing peptide	BC024515	1424525_at	4.9436426	3.00588E-05	2.752845903	5.72954E-07
sortilin-related VPS10 domain containing receptor 3	AK018111	1425111_at	4.885766	1.03645E-05	1.29051599	0.029733649
dopamine receptor D1A	BE957273	1455629_at	4.869493	3.77525E-05	1.815881979	0.000516498
proprotein convertase subtilisin/kexin type 5	BB241731	1437339_s_at	0.210528027	7.83039E-05	0.574126078	9.15496E-05
interleukin 1 receptor, type I	NM_008362	1448950_at	0.210572243	9.64524E-06	0.241135352	2.79816E-08

Acknowledgements

We thank Dr. Yoko Nabeshima at Kyoto University for her instruction on the dissection technique and Ms. Aki Miyakawa at Fujita Health University for her support to film. This work was supported by the Program for Promotion of Fundamental Studies in Health Sciences of the National Institute of Biomedical Innovation, a Grant-in-Aid for Scientific Research on Priority Areas -Integrative Brain Research (Shien)- from MEXT in Japan, and by a Grant-in-Aid from CREST of the Japan Science and Technology Agency.

References

1. Yamasaki, N., Maekawa, M., Kobayashi, K., Kajii, Y., Maeda, J., Soma, M., Takao, K., Tanda, K., Ohira, K., Toyama, K., Kanzaki, K., Fukunaga, K., Sudo, Y., Ichinose, H., Ikeda, M., Iwata, N., Ozaki, N., Suzuki, H., Higuchi, M., Suhara, T., Yuasa, S. & Miyakawa, T. Alpha-CaMKII deficiency causes immature dentate gyrus, a novel candidate endophenotype of psychiatric disorders. *Mol. Brain* **1**, 6 (2008).
2. Insausti, A. M., Megias, M., Crespo, D., Cruz-Orive, L. M., Dierssen, M., Vallina, I. F., Insausti, R. & Florez, J. Hippocampal volume and neuronal number in Ts65Dn mice: a murine model of Down syndrome. *Neurosci. Lett.* **253**, 175 (1998).

3. Redwine, J. M., Kosofsky, B., Jacobs, R. E., Games, D., Reilly, J. F., Morrison, J. H., Young, W. G. & Bloom, F. E. Dentate gyrus volume is reduced before onset of plaque formation in PDAPP mice: a magnetic resonance microscopy and stereologic analysis. *Proc. Natl. Acad. Sci. U.S.A.* **100**, 1381 (2003).
4. Lein, E. S., Zhao, X. & Gage, F. H. Defining a molecular atlas of the hippocampus using DNA microarrays and high-throughput in situ hybridization. *J. Neurosci.* **24**, 3879 (2004).
5. Matsuo, N., Yamasaki, N., Ohira, K., Takao, K., Toyama, K., Eguchi, M., Yamaguchi, S. & Miyakawa, T. Neural activity changes underlying the working memory deficit in alpha-CaMKII heterozygous knockout mice. *Front. Behav. Neurosci.* **3**, 20 (2009).
6. Franklin, K. B. J. & Paxinos, G. The Mouse Brain in Stereotaxic Coordinates. *Academic Press, Inc.: San Diego* (1997).

